Mode-coupling theory and simulation results for the "running-sandpile" model of self-organized criticality

Pui-Man Lam* and Fereydoon Family
Department of Physics, Emory University, Atlanta, Georgia 30322
(Received 29 May 1992)

We examine the model of self-organized criticality investigated by Hwa and Kardar [Phys. Rev. Lett. **62**, 1813 (1989)] based on a continuum, nonlinear driven diffusion equation with stochastic noise. We point out some problems in the heuristic arguments used in relating the temporal response functions of the model to the exponents calculated exactly by dynamic-renormalization-group analysis. We propose an alternative, direct calculation of the response function and its power spectrum for the total energy dissipated in the system by a mode-coupling theory, making use of the renormalization-group recursion relations for the renormalized parameters of the theory. We find a significant difference from the previous results. Simulation results of the "running-sandpile" model agree with our mode-coupling-theory predictions.

PACS number(s): 05.60.+w, 05.40.+j, 64.60.Ht

I. INTRODUCTION

The phenomena of self-organized criticality is a topic of intense recent interest. As suggested by Bak, Tang, and Wiesenfeld [1,2], it relates scale invariances in spatial and temporal domains. Spatial scaling invariances are characterized by fractal geometry, while temporal scale invariances are manifested by $1/\omega^{\alpha}$ power spectra. Most of the models studied so far are cellular automata or sandpile models [1–4], which, starting from an arbitrary initial state, evolve automatically into a critical state characterized by power-law correlations in both spatial and temporal scales. The name "self-organized criticality" comes from the lack of a tuning parameter such as the temperature in second-order phase transitions.

Hwa and Kardar [5] recently developed a continuum model of self-organized criticality. Based on considerations of symmetry and conservation laws in sandpile models, they have constructed a nonlinear driven diffusion equation in the presence of stochastic noise to describe self-organized critical phenomena. A one-loop dynamic-renormalization-group analysis was applied to calculated the dynamic exponents z, roughening exponent χ, and the spatial anisotropy exponent ζ for this model. These exponents are actually exact because of nonrenormalization of the noise spectrum and Galilean invariance. A heuristic argument was used to relate the temporal correlations $g_J(t)\equiv\langle J(t)J(0)\rangle$ of the total output current $J(t)$ and $g_E(t)\equiv\langle E(t)E(0)\rangle$ of the total energy $E(t)$ dissipated throughout the system, in terms of the exponents z, ζ, and χ. The resulting power spectra for total current correlations $S_J(\omega)$ and the total-energy correlation $S_E(\omega)$ have the forms $S_J(\omega)\sim\omega^{-\alpha_J}$ and $S_E(\omega)\sim\omega^{-\alpha_E}$, with $\alpha_J=1/z$ and $\alpha_E=2/z$, respectively. In this paper we want to point out some problems in the heuristic arguments used in Ref. [5] to relate these temporal correlations to the exponents z, ζ, and χ. In addition, we calculate the temporal correlation $g_E(t)$ directly by applying the mode-coupling theory [6–9], starting from a linearized theory and making use of the known renormalization-group recursion relations for the renormalized parameters in the nonlinear theory. Our results for the exponents α_E differ significantly from those of Hwa and Kardar.

Very recently, Hwa and Kardar [10] proposed a "running-sandpile" model, in which sand grains are added at a constant rate from the outside and the avalanches are allowed to collide and coalesce. This "running"-sandpile model differs from the original Bak, Tang, and Wiesenfeld model, in which the input current is zero in the large-system limit. We have simulated this running-sandpile model and the result seems to support our model-coupling-theory predictions.

In Sec. II we will briefly review the model of Hwa and Kardar, the dynamic-renormalization-group results for the renormalized parameters, and the heuristic arguments of Hwa and Kardar to relate the temporal response functions to the exact exponents. We will point out some problems with these arguments. In Sec. III we will discuss the mode-coupling theory for the calculation of the total-energy response function starting from a linearized theory and making use of the known renormalization-group recursion relations for the renormalized parameter in the nonlinear theory. Some details of the calculations are relegated to an appendix. In Sec. IV we present our simulation results of a running-sandpile model [10] in $d'=2$ dimensions, where the spatial dimension d is $d'+1$. This running-sandpile model, rather than the original sandpile model of Bak, Tang, and Wiesenfeld, is supposed to correspond to the continuum model of Hwa and Kardar [5]. The results of these simulations seem to support our mode-coupling-theory predictions. Section V contains our discussions and conclusions.

II. DYNAMIC RENORMALIZATION GROUP FOR SELF-ORGANIZED CRITICALITY

In this section we will briefly review the theory of Hwa and Kardar. We will not repeat their symmetry and conservation law considerations in deriving the nonlinear driven diffusion equation, but will simply start with this equation itself [5]:

$$\frac{\partial h}{\partial t}=\nu_{\parallel}\partial_{\parallel}^2 h+\nu_{\perp}\nabla_{\perp}^2 h-\frac{\lambda}{2}\partial_{\parallel}h^2+\eta(\mathbf{x},t)\ . \tag{1}$$

The height function $h(\mathbf{x},t)$ is defined as a deviation from the flat steady-state sand profile. The component of gravity parallel to the surface picks out a direction of transport $\hat{\mathbf{T}}$. Let $\mathbf{x}_{\parallel}\equiv(\hat{\mathbf{T}}\cdot\mathbf{x})\hat{\mathbf{T}}$ and $\mathbf{x}_{\perp}\equiv\mathbf{x}-\mathbf{x}_{\parallel}$. The first two terms on the right of (1) describe relaxation of the height through surface tension (the Laplacian term is split into parts parallel and perpendicular to the transport direction $\hat{\mathbf{T}}$). The third term is present due to the absence of $\mathbf{x}_{\parallel}\rightarrow-\mathbf{x}_{\parallel}$ symmetry and hence related to the presence of transport, and η represents a stochastic noise. Equation (1) is invariant under the joint inversion symmetry $h\rightarrow-h$ and $\mathbf{x}_{\parallel}\rightarrow-\mathbf{x}_{\parallel}$. In the absence of noise, there is a local height-conservation law and a transport current $\mathbf{j}(\mathbf{x},t)$ satisfying $\partial_t h+\nabla\cdot\mathbf{j}=0$, where

$$\mathbf{j}=-\nu_{\perp}\nabla_{\perp}h-\nu_{\parallel}\partial_{\parallel}h\hat{\mathbf{T}}+\frac{\lambda}{2}h^2\hat{\mathbf{T}}\ . \tag{2}$$

The stochastic noise has the properties $\langle\eta\rangle=0$ and

$$\langle\eta(\mathbf{x},t)\eta(\mathbf{x}',t')\rangle=2D\delta^{d'}(\mathbf{x}-\mathbf{x}')\delta(t-t')\ . \tag{3}$$

Here d' is the spatial dimension of the surface described by $\mathbf{x}=(\mathbf{x}_{\parallel},\mathbf{x}_{\perp})$, and the spatial dimension of the system $d=d'+1$.

The exponents z, ζ, and χ are defined through the homogeneous scaling transformation

$$h(\mathbf{x}_{\parallel},\mathbf{x}_{\perp},t)=b^{\chi}h(\mathbf{x}_{\parallel}/b,\mathbf{x}_{\perp}/b^{\zeta},t/b^{z})\ , \tag{4}$$

with a scaling factor $b\equiv e^{l}\geq 1$.

Hwa and Kardar [5] had performed a dynamic-renormalization-group calculation on (1). For $d'<4$, the terms in the perturbation series diverge due to the infrared limit of momentum integrations. For $d'\geq 4$, the perturbation series diverges also in the ultraviolet. This is taken care of by introducing two large momentum cutoffs $\Lambda_{\parallel}$ and $\Lambda_{\perp}$, in the two directions. The infrared divergences are circumvented by integrating out only momenta in an outer shell $\Lambda_{\parallel}/b<q_{\parallel}<\Lambda_{\parallel}$ and $\Lambda_{\perp}/b<|q_{\perp}|<\Lambda_{\perp}$, where $l=\ln b\ll 1$ is the infinitesimal shell thickness. The remaining modes are inflated back to the original size by the scaling transformation (4). The rescaled modes obey (1) with renormalized parameters satisfying recursion relations of the form

$$\frac{d\nu_{\parallel}}{dl}=\nu_{\parallel}\left[z-2+u\,\pi\frac{7-d'}{32}\right]\ , \tag{5a}$$

$$\frac{d\nu_{\perp}}{dl}=\nu_{\perp}(z-2\zeta)\ , \tag{5b}$$

$$\frac{d\lambda}{dl}=\lambda(z+\chi-1)\ , \tag{5c}$$

$$\frac{dD}{dl}=D[z-2\chi+(1-d')\zeta-1]\ , \tag{5d}$$

where $u=[2S_{d'-1}/(2\pi)^{d'}][\lambda^2 D/(\nu_{\parallel}\nu_{\perp})^{3/2}]$ is the effective coupling constant ($S_{d'}$ being the surface area of a unit d'-dimensional sphere). From (5), the recursion relation for u follows:

$$\frac{du}{dl}=u\left[(4-d')\zeta-\frac{7-d'}{2}\frac{3\pi}{32}u\right]\ . \tag{5e}$$

The recursion relations (5b) to (5d) are just those of homogeneous scaling. Only the parameter $\nu_{\parallel}$ is renormalized. The nonrenormalization of $\nu_{\perp}$ and D come from the fact that the nonlinearity in (1) is proportional to the *external* momentum $\mathbf{k}_{\parallel}$. The nonrenormalization of λ is due to the invariance of (1) under the Galilean transformation: $x_{\parallel}\rightarrow x_{\parallel}-\epsilon\lambda t$, $t\rightarrow t$, and $h\rightarrow h+\epsilon x_{\parallel}$. From Eqs. (5), the exponents are determined exactly:

$$z=\frac{6}{7-d'}\ ,\quad \chi=\frac{1-d'}{7-d'}\ ,\quad \zeta=\frac{3}{7-d'}\ . \tag{6}$$

To make connection with $1/f$ noise, Hwa and Kardar consider the frequency dependence of some macroscopic response functions. A natural choice is the total output current $J(t)=\int d^{d'-1}x_{\perp}j(L_{\parallel},\mathbf{x}_{\perp},t)$ with integration at the system edge at $x_{\parallel}=L_{\parallel}$. From (2), the cumulant $\langle j(\mathbf{x}_{\parallel},\mathbf{x}_{\perp},t)j(\mathbf{x}_{\parallel},0,0)\rangle_c$ is given by

$$\langle j(\mathbf{x}_{\parallel},\mathbf{x}_{\perp},t)j(\mathbf{x}_{\parallel},0,0)\rangle_c\sim\langle h^2(\mathbf{x}_{\parallel},\mathbf{x}_{\perp},t)h^2(\mathbf{x}_{\parallel},0,0)\rangle_c\ . \tag{7}$$

Here the term cumulant means the connected part with the product terms of lower order subtracted off. In the current density j only the dominant term has been taken into account. Using the scaling form (4) for h, we have

$$\langle j(\mathbf{x}_{\parallel},\mathbf{x}_{\perp},t)j(\mathbf{x}_{\parallel},0,0)\rangle_c\sim|\mathbf{x}_{\perp}|^{4\chi/\zeta}f(t/|\mathbf{x}_{\perp}|^{z/\zeta}\ . \tag{8}$$

Notice that (8) holds only asymptotically, i.e., for large values of $|\mathbf{x}_{\perp}|$. Let us denote the range of $|\mathbf{x}_{\perp}|$ beyond which (8) holds as R, then we have

$$\langle J(t)J(0)\rangle=\int_0^R d^{d'-1}x_{\perp}\langle j(\mathbf{x}_{\parallel},\mathbf{x}_{\perp},t)j(\mathbf{x}_{\parallel},0,0)\rangle + A\int_R^{\infty}d^{d'-1}x_{\perp}|x_{\perp}|^{4\chi/\zeta}f(t/|x_{\perp}|^{z/\zeta})\ , \tag{9}$$

where A is a proportionality constant. If we assume $R=0$, then we have from (9)

$$\langle J(t)J(0)\rangle\sim\int_0^{\infty}|\mathbf{x}_{\perp}|^{4\chi/\zeta}f(t/|\mathbf{x}_{\perp}|^{z/\zeta})|\mathbf{x}_{\perp}|^{d'-2}dx_{\perp}\ . \tag{10}$$

Changing the variable of integration to $y=t/|x_{\perp}|^{z/\zeta}$, we obtain

$$\langle J(t)J(0)\rangle_c\sim t^{[4\chi+(d'-1)\zeta]/z}\ . \tag{11}$$

Substituting the values of the exponents (6) we have $\langle J(t)J(0)\rangle_c\sim t^{(1/z)-1}$. Fourier transforming this, we have

$$S_J(\omega)\sim\int t^{(1/z)-1}e^{i\omega t}dt=\int\left[\frac{x}{\omega}\right]^{(1/z)-1}e^{ix}\frac{dx}{\omega}\sim\omega^{-1/z}\ . \tag{12}$$

This gives the exponent α_J, defined by $S_J(\omega)\sim\omega^{-\alpha_J}$ as $\alpha_J=1/z$.

Similarly, for the total energy $E(t)$ dissipated throughout the system at time t, we have $E(t)\sim\int d^{d'}x h^2(\mathbf{x}_\parallel,\mathbf{x}_\perp,t)$. Using the same procedure as before, we find for the response function

$$g_E(t)=\langle E(t)E(0)\rangle\sim t^{[4\chi+(d'-1)\zeta+1]/z}\ . \tag{13}$$

Using the values of the exponents given in (6) we find $g_E(t)\sim t^{(2/z)-1}$. Taking the Fourier transform, we have

$$S_E(\omega)\sim\int t^{(2/z)-1}e^{i\omega t}dt\sim\omega^{-2/z}\ . \tag{14}$$

The exponent α_E defined by $S_E(\omega)\sim\omega^{-\alpha_E}$ is then given by $\alpha_E=2/z$.

At first sight, the heuristic arguments of Hwa and Kardar given above, which yield the relations between α_J, α_E, and z, seem to be fine. However, as we look more closely, we find that there are problems. Using (6) we find for the exponent in the integrand of (12) to be $(1/z)-1=0$, $-\frac{1}{6}$, $-\frac{1}{3}$, and $-\frac{1}{2}$, respectively, for $d'=1$, 2, 3, and 4. Since this exponent is negative, the Fourier transform defined in (12) exists and there is no problem. For the exponent in the integrand of (14), however, we find $(2/z)-1=1$, $\frac{2}{3}$, $\frac{1}{3}$, and 0, respectively, for $d'=1$, 2, 3, and 4. Since this exponent is positive, the Fourier transform (14) is not defined. Therefore the relation $\alpha_E=2/z$ is in doubt. Also we believe that the temporal correlation function $g_E(t)$, which *increases* with time, is not physical. We think the problem can be traced back to the assumption $R=0$ in (9) to obtain (10), from which (11) and (13) follow.

III. MODE-COUPLING THEORY

In this section we will describe a direct calculation of the response function $g_E(t)$ within the mode-coupling theory. We start with the linearized version of (1):

$$\frac{\partial h}{\partial t}=\nu_\parallel\partial_\parallel^2 h+\nu_\perp\nabla_\perp^2 h+\eta(\mathbf{x},t)\ . \tag{15}$$

Defining the Fourier transform of $h(\mathbf{x}_\parallel,\mathbf{x}_\perp,t)$ as

$$h(\mathbf{x}_\parallel,\mathbf{x}_\perp,t)=\frac{1}{(2\pi)^{d'}}\int dk_\parallel d^{d'-2}k_\perp\hat{h}(\mathbf{k}_\parallel,\mathbf{k}_\perp,t)e^{ik_\parallel x_\parallel}e^{i\mathbf{k}_\perp\cdot\mathbf{x}_\perp}\ , \tag{16}$$

Eq. (15) can be written as

$$\frac{\partial\hat{h}}{\partial t}=-\nu_\parallel k_\parallel^2\hat{h}-\nu_\perp k_\perp^2\hat{h}+\hat{\eta}(k_\parallel,\mathbf{k}_\perp,t)\ . \tag{17}$$

The solution of (17) has the form

$$\hat{h}(k_\parallel,\mathbf{k}_\perp,t)=e^{-(\nu_\parallel k_\parallel^2+\nu_\perp k_\perp^2)t}\int_0^t ds\, e^{(\nu_\parallel k_\parallel^2+\nu_\perp k_\perp^2)s}\hat{\eta}(k_\parallel,\mathbf{k}_\perp,s)\ . \tag{18}$$

We will only be interested in the response function $g_E(t)$, which is easier to calculate than the function $g_J(t)$ within the framework of mode-coupling theory. For $g_E(t)$ we have

$$\begin{aligned}g_E(\tau)&=\int d^{d'}x d^{d'}y\langle h^2(\mathbf{x},t)h^2(\mathbf{y},t')\rangle_c\\&=\sum_{\mathbf{k},\mathbf{q}}\langle|\hat{h}(\mathbf{k},t)|^2|\hat{h}(\mathbf{q},t')|^2\rangle_c\ ,\end{aligned} \tag{19}$$

where $\tau\equiv|t-t'|$.

Using the solution (18) for $\hat{h}$ and the noise spectrum in $\mathbf{k}$ space

$$\langle\hat{\eta}(\mathbf{k},t)\hat{\eta}(\mathbf{k}',t')\rangle=2D\delta^{d'}(\mathbf{k}+\mathbf{k}')\delta(t-t')\ , \tag{20}$$

we obtain the expression for $g_E(\tau)$ in the limit $t,t'\to\infty$, $t>t'$, $\tau=t-t'$ finite, and $k_0=1/L$ finite, where L is the linear size of the system (see Appendix):

$$g_E(\tau)=D^2\left[\frac{L}{2\pi}\right]^{d'}S_{d'-1}\int_{k_0}^\infty dk\, k^{d'-1}\int_0^{\pi/2}d\theta\frac{\sin^{d'-2}\theta}{k^4(\nu_\parallel\cos^2\theta+\nu_\perp\sin^2\theta)^2}e^{-2k^2\tau(\nu_\parallel\cos^2\theta+\nu_\perp\sin^2\theta)}\ . \tag{21}$$

The power spectrum $S_E(\omega)$ is given by the real part of the Fourier transform of (21). We obtain for $d'\geq 2$,

$$S_E(\omega)=-2D^2\left[\frac{L}{2\pi}\right]^{d'}S_{d'-1}\int_{k_0}^\infty dk\, k^{d'-1}\int_0^{\pi/2}d\theta\frac{\sin^{d'-2}\theta}{k^2(\nu_\parallel\cos^2\theta+\nu_\perp\sin^2\theta)}\frac{1}{\omega^2+4k^4(\nu_\parallel\cos^2\theta+\nu_\perp\sin^2\theta)^2}\ . \tag{22}$$

For $d'=4$, (21) becomes

$$g_E(\tau)=D^2\left[\frac{L}{2\pi}\right]^{d'}S_3\int_0^{\pi/2}d\theta\frac{\sin^2\theta}{(\nu_\parallel\cos^2\theta+\nu_\perp\sin^2\theta)^2}\int_{k_0}^\infty\frac{dk}{k}e^{-2k^2\tau(\nu_\parallel\cos^2\theta+\nu_\perp\sin^2\theta)}\ . \tag{23}$$

The k integral diverges logarithmically at the upper limit as $\tau\to 0$. Therefore for $d'=4$, $g_E(\tau)\sim\ln\tau$, for $\tau\to 0$. This is in agreement with the result $(2/z)-1=0$ at $d'=4$ of Hwa and Kardar but only in the limit $\tau\to 0$. For finite τ, $g_E(\tau)$ is finite and we find numerically that it decreases monotonically with τ.

For $d'=4$, the k integral in (22) can be performed analytically. We find

$$S_E(\omega)=-\tfrac{1}{2}D^2\left[\frac{L}{2\pi}\right]^{d'}S_{d'-1}\frac{1}{\omega}\int_0^{\pi/2}d\theta\frac{\sin^2\theta}{(\nu_\parallel\cos^2\theta+\nu_\perp\sin^2\theta)^2}\left\{\frac{\pi}{2}-\tan^{-1}\left[\frac{2k_0^2(\nu_\parallel\cos^2\theta+\nu_\perp\sin^2\theta)}{\omega}\right]\right\}. \tag{24}$$

This gives $S_E(\omega)\sim 1/\omega$ for $d'=4$ and large ω, in agreement with the result of Hwa and Kardar. We have also evaluated the double integral in (22) numerically and verified the result $\alpha_E=1$ for $d'=4$ to high accuracy.

For $d'<4$, the form of the response function (21) and that of the power spectrum (22) for the linear theory can be used to obtain the corresponding quantities for the nonlinear model within the mode-coupling approximation by rewriting (21) and (22) in the forms [6–9]:

$$g_E(\tau)=S_{d'-1}\left[\frac{L}{2\pi}\right]^{d'}\int_{k_0}^{\infty}k^{d'-1}dk\int_0^{\pi/2}\frac{\sin^{d'-2}\theta D^2(k)d\theta}{k^4(\nu_\parallel(k)\cos^2\theta+\nu_\perp(k)\sin^2\theta)^2}e^{-2k^2\tau[\nu_\parallel(k)\cos^2\theta+\nu_\perp(k)\sin^2\theta]}, \tag{25}$$

$$S_E(\omega)=-2\left[\frac{L}{2\pi}\right]^{d'}S_{d'-1}\int_{k_0}^{\infty}k^{d'-1}dk\int_0^{\pi/2}\frac{\sin^{d'-2}\theta D^2(k)d\theta}{k^2[\nu_\parallel(k)\cos^2\theta+\nu_\perp(k)\sin^2\theta]}\frac{1}{\omega^2+4k^4[\nu_\parallel(k)\cos^2\theta+\nu_\perp(k)\sin^2\theta]^2}. \tag{26}$$

The scale-dependent parameters $D(b)$, $\nu_\parallel(b)$, and $\nu_\perp(b)$ can be obtained by solving the recursion relations (5a) to (5e) for these parameters as a function of the scaling factor b and by making the substitution $b\to(1/k\cos\theta)$. Using (6) for the exponents z, χ, and ζ, the solutions of the recursion relations have the form:

$$\nu_\perp(b)=\nu_\perp^B,\quad D(b)=D^B,\quad \lambda(b)=\lambda^B, \tag{27}$$

$$\nu_\parallel=\nu_\parallel^B b^{z-2}\left\{\frac{(4-d')\zeta+\frac{7-d'}{2}\frac{3\pi}{32}u^B[b^{(4-d')\zeta}-1]}{(4-d')\zeta}\right\}^{2/3}, \tag{28}$$

where $\nu_\parallel^B$, $\nu_\perp^B$, λ^B, and u^B are bare values of these parameters. Making the replacement $b\to 1/(k\cos\theta)$ in (28) and substituting these equations into (26) we find by numerical evaluation of the double integral that to very high accuracy, $S_E(\omega)\sim\omega^{-\alpha_E}$, with $\alpha_E=1.95$ for $d'=2$ and $\alpha_E=1.54$ for $d'=3$. We have checked that these results are independent of L and the values of the bare parameters. For $d'=1$, the double integrals in (24) reduce to a single integral and we find $\alpha_E=2$ for that case, in agreement with Hwa and Kardar. But for $d'=2$ and $d'=3$ our results for α_E differ significantly from theirs ($2/z=\frac{7}{3}=1.67$, 1.33 for $d'=2,3$).

Similarly, Eq. (25) can be used to obtain $g_E(\tau)$ for the nonlinear model by substituting the k dependence of $\nu_\parallel$ into it and carrying out the integration. We find that $g_E(\tau)$ is a monotonic decreasing function of τ for all d', as expected.

IV. SIMULATION OF A "RUNNING-SANDPILE" MODEL

Hwa and Kardar have suggested [10] that the continuum model (1) describes a running-sandpile model in which the avalanches can interact and coalesce. This is different from the original sandpile model of Bak, Tang, and Wiesenfeld (BTW) in which sand grains are added one at a time and the system is allowed to completely relax between additions. In the running-sandpile model, there is a finite input current $J_{\rm in}$ of sand grains per unit time. For a system of $L\times L$ sites in $d'=2$ dimensions, the probability per site of depositing a particle is taken to be $p=J_{\rm in}/L^2$ per unit time. In the original BTW model, the input current $J_{\rm in}$ is zero in the infinite system limit. In the running-sandpile model we sweep through every site of the lattice and deposit a particle with a probability p depending on the size of the system as given above, in one time unit. Simultaneously within this same time unit we sweep through every site of the lattice and apply the BTW sandpile relaxation rules to any site which has a "slope" Z above the critical value Z_c

$$Z(x,y)\to Z(x,y)+1 \text{ with probability } p \tag{29a}$$

$$\begin{aligned}&Z(x,y)\to Z(x,y)-4,\\ &Z(x+1,y)\to Z(x+1,y)+1,\\ &Z(x-1,y)\to Z(x-1,y)+1,\quad Z(x,y)>Z_c,\\ &Z(x,y+1)\to Z(x,y+1)+1,\\ &Z(x,y-1)\to Z(x,y-1)+1,\end{aligned} \tag{29b}$$

where (x,y) denotes the coordinates of a point on the square lattice. At the boundary of the system $Z(\text{boundary})=0$ at all times. This corresponds to the open boundary condition, where sands fall off the edge of the system. After every site in the system has been relaxed once by applying the results (29b) successively once for every site, the time is increased by one unit. Irrespective of whether all the sites in the system have relaxed to a value below or at the critical value Z_c, in the next time unit sand grains are again deposited at every site with probability p and the process continues. Here is where the running-sandpile model differs from the original BTW model. In the BTW model, sand grains are added only after the system has relaxed to a situation where all $Z(x,y)$ are below or at the critical value z_c. The additional of sand grains from outside at a constant rate in the running-sandpile model provides an external clock. In the BTW model time is not well defined since the interval between sand additions varies.

The physical quantities that we measure are the

response functions for the sand current $J(t)$ flowing out of the system and the total-energy dissipation $E(t)$, or the total number of relaxation processes via (29b), at time t. Starting from any initial configuration for the "slope" $Z(x,y)$, the system is run for a sufficient length of time t_0 until the steady state has been reached. This can be most easily checked by calculating the average $\langle Z(x,y)\rangle$ and the fluctuations $\langle \Delta Z^2\rangle$ defined by $\langle Z\rangle = L^{-2}\sum_{x,y} Z(xy)$, $\langle \Delta Z^2\rangle = \langle Z^2\rangle - \langle Z\rangle^2$, and $\langle Z^2\rangle = L^{-2}\sum_{x,y} Z^2(x,y)$, as a function of the time t until these quantities become constant in time. Then we start calculating the response functions defined by

$$g_X(\tau) \equiv T^{-1}\int_{t_0}^{T} X(t+\tau)X(t)dt \ , \tag{30}$$

where T is some period of time much larger than t_0 and X denotes either the current $J(t)$ flowing out of the system or the total-energy dissipation $E(t)$ at time t. The current $J(t)$ can be calculated by counting the number of occurrences of (29b) right next to the boundary of the system at time t and total-energy dissipation $E(t)$ can be calculated by counting the total number of occurrences of (29b) in the whole system at time t. The power spectrum is given by the cosine Fourier transform of the response functions

$$S_X(\omega) = \int g_X(\tau)\cos\omega\tau \, d\tau \ . \tag{31}$$

In Fig. 1 we show the power spectrum $S_J(\omega)$ for the current $J(t)$ in a log-log plot with the input current fixed at $J_{\text{in}}=0.5$ and system size $L=80$ for $d'=2$. The dashed lines indicate the regions in the spectrum where the log-log plot shows a linear behavior. In this figure we can identify three regions as predicted in Ref. [10] and found in one-dimensional simulations by the same authors. In the high-frequency region, which corresponds to short-time scales, we find the exponent $\beta_J \simeq 0.77$ defined by $S_J(\omega)\sim\omega^{-\beta_J}$. In this short-time-scales region collisions of avalanches are negligible and we have the sandpile model of BTW. In the intermediate frequency region corresponding to intermediate time scales, collisions of avalanches are important and we find the exponent $\alpha_J \simeq 0.31$ defined by $S_J(\omega)\sim\omega^{-\alpha_J}$. At very long time scales, which correspond to the low-frequency region, we find that the power spectrum increases with frequency. This is the region of "great event" as found in Ref. [10], in which the sandpile exhibits systemwide discharge events and corresponds to a region of anticorrelations. Our results are too rough to estimate the exponent ψ defined by $S_J(\omega)\sim\omega^{+\psi}$ in this frequency range and predicted in mean-field theory to be $\psi=\frac{1}{2}$ [10].

The different scaling regimes are seen more clearly in the power spectrum $S_E(\omega)$ of the total energy, shown in Fig. 2 for $d'=2$. This shows a log-log plot of the total-energy spectrum at fixed input current $J_{\text{in}}=0.5$ and system sizes $L=80$. The dashed lines indicate the regions in the spectrum where the log-log plot shows linear behavior. Again three regions can be identified. At high frequencies, which correspond to small-time scales for which collisions among avalanches are negligible, we find the exponent β_E defined by $S_E(\omega)\sim\omega^{-\beta_E}$, to be $\beta_E \simeq 1.5$, which is close to the value of BTW [1,2]. At intermediate frequencies, which correspond to intermediate time scales, collisions among avalanches are important and we find the exponent α_E defined by $S_E(\omega)\sim\omega^{-\alpha_E}$, to be increasing with system size. For the largest system that we have simulated, $L=80$, we find $\alpha_E=1.85$. This value of α_E differs from Hwa and Kardar's estimate of 1.67 and is close to our mode-coupling-approximation result of 1.95

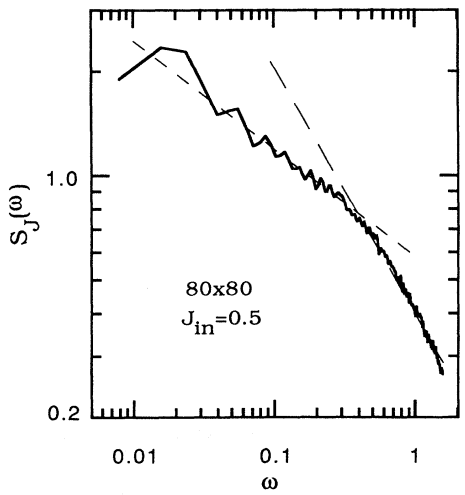

FIG. 1. Double logarithmic plot of the power spectrum $S_J(\omega)$ for the current response function at input current $J_{\text{in}}=0.5$ and system size 80×80. The dashed lines indicate linear regions with slopes -0.31 and -0.77 at intermediate and large frequencies, respectively.

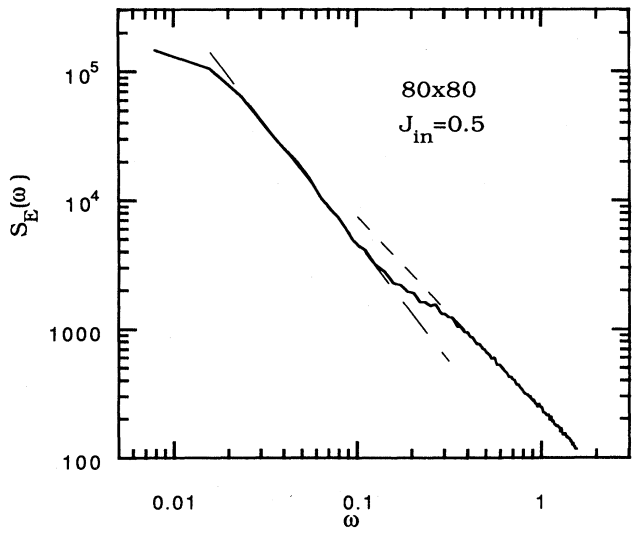

FIG. 2. Double logarithmic plot of the power spectrum $S_E(\omega)$ for the total-energy response function at input current $J_{\text{in}}=0.5$ and system size 80×80. The dashed lines indicate linear regions with slopes -1.85 and -1.50 at intermediate and large frequencies, respectively.

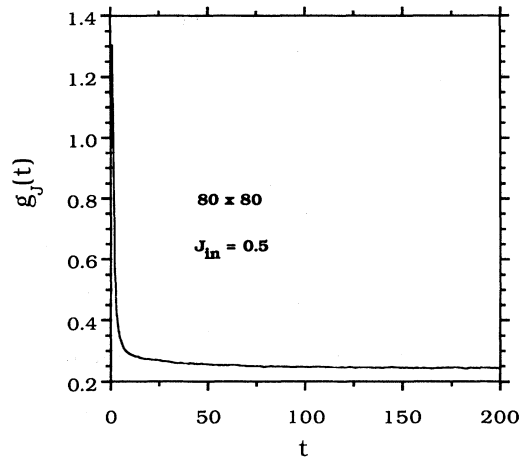

FIG. 3. The current-current response function $g_J(t)$ vs time t for input current $J_{in}=0.5$ and system size 80×80.

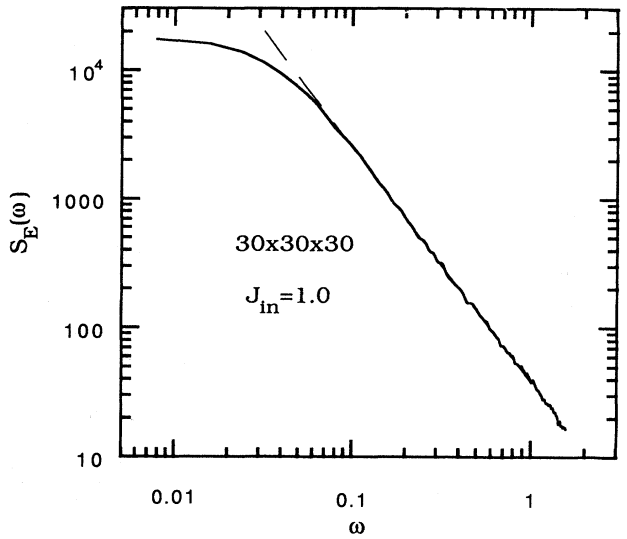

FIG. 5. Double logarithmic plot of the power spectrum $S_E(\omega)$ for the total-energy response function at input current $J_{in}=1.0$ and system size $30\times30\times30$. The dashed line indicates linear region with slope -1.82.

at $d'=2$. The very low frequency or long-time behavior of $S_E(\omega)\sim\omega^{+\psi}$ is seen only for small system sizes. This is because the response function $g_J(t)$ approaches its asymptotic, long-time behavior at much larger time t than for the response function $g_J(t)$, and for larger system size, one has to go to even longer time t to approach the asymptotic behavior.

In Fig. 3 we show the current response function $g_J(t)$ for input current $J_{in}=0.5$ and system sizes $L=80$. We see that the asymptotic value of 0.25 is obtained very rapidly as the time t increases. The asymptotic value of $\frac{1}{4}$ is consistent with the fact that in the steady state, the average output current must be the same as the input current $\langle J(t)\rangle=J_{in}$. In Fig. 4 we show the total-energy response function $g_E(t)$ for input current $J_{in}=0.5$ and system sizes $L=80$. In contrast to the current response function, we see that the total-energy response function $g_E(t)$ has barely reached an asymptotic value at the maximum time of about 200. That is the reason why we do not see the very small frequency great event region in the power spectrum $S_E(\omega)$, except for small system sizes. To see the great event region in $S_E(\omega)$ one has to go to much longer times in the total-energy response function than is done here.

The above results are obtained for $d'=2$. For $d'=3$ we have simulated a $30\times30\times30$ system. In Fig. 5 we show the log-log plot of the power spectrum $S_E(\omega)$ for the total-energy response function, for input current $J_{in}=1.0$. At this value of the input current, the slope of

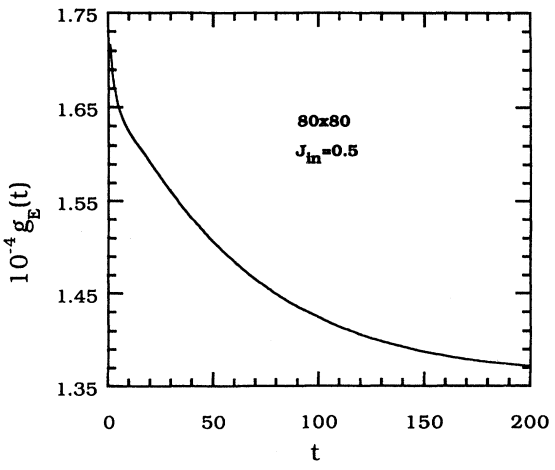

FIG. 4. Same as Fig. 3, but for the total-energy response function $g_E(t)$.

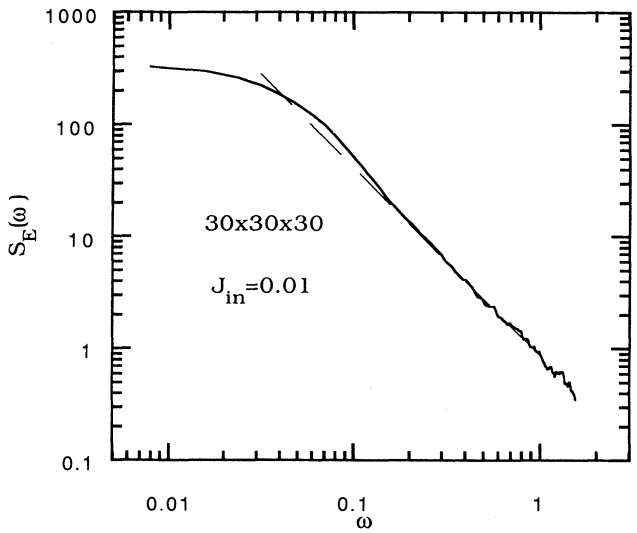

FIG. 6. Double logarithmic plot of the power spectrum $S_E(\omega)$ for the total-energy response function at input current $J_{in}=0.01$ and system size $30\times30\times30$. The dashed line indicates linear region with slope -1.64.

the curve is about -1.8 compared with the prediction of -1.54 of the mode-coupling theory. In Fig. 6 we show the log-log plot of the power spectrum $S_E(\omega)$ for the total-energy response function for input current $J_{\text{in}}=0.01$. The slope of the curve is about -1.60. This is quite different from the value at $J_{\text{in}}=1.0$. So in $d'=3$ there is again qualitative evidence for a crossover behavior of α_E from the noninteracting avalanches limit to the interacting avalanches limit. In higher dimensions, the average avalanche duration is larger. Therefore one has to use a much smaller input current in order for the avalanches not to interact. A very small J_{in} would require much longer running time to get the same statistics.

V. DISCUSSIONS AND CONCLUSIONS

We have presented a mode-coupling-approximation calculation for the exponent α_E of a continuum model of self-organized criticality proposed by Hwa and Kardar [5]. The result of our calculation for the exponent α_E characterizing the power spectrum for total-energy response function differs significantly from the result of Hwa and Kardar in $d'=2$ and 3. As shown in the Appendix, in the mode-coupling theory we have taken anisotropy of the system into account by separating k into $k_\parallel$ and $k_\perp$ and by replacing b by $1/(k\cos\theta)$. We have simulated a running-sandpile model proposed by Hwa and Kardar [10] to be described by their continuum model for a system with open boundaries on the square lattice. The results of our simulations give $\alpha_E\simeq 1.9$, which is quite different from the Hwa-Kardar prediction of $\alpha_E\simeq 1.67$, and seem to support our mode-coupling-approximation results in the interacting-avalanches regime.

Although the mode-coupling theory is in principle an uncontrolled approximation, it has been known to give good results in other applications [7,9]. It has been known to give good results in the velocity-velocity correlation function of the random-force driven Burger equation [7], as well as in universal scaling functions and amplitude ratios in surface growth problems [9].

Finally we would like to point out that the running-sandpile model described above was also studied by Jensen, Christensen, and Fogedby [11], in which one finds the following statement in the next to the last paragraph of their paper: we simply continuously add sand randomly (in time and space) at a *constant rate* and let the model evolve according to the updating algorithm. In their model they did not find a crossover behavior in α_E but instead found that $\alpha_E\simeq 2.0$, which is close to our mode-coupling result of 1.95. From this they concluded that the Bak, Tang, and Wiesenfeld sandpile model has a $1/f^2$ power spectrum in $d'=2$ dimensions. From our results we believe that they had probably used an input current J_{in}, which is too large, so that they are in the region in which the avalanches always interact. In their figure caption for their power spectrum it is stated that the probability for adding sand at one site is 0.05 per time step. This value of the probability is about three orders of magnitude larger than our value of $0.5/(80)^2$.

ACKNOWLEDGMENTS

This research was supported by the Office of Naval Research. We would like to thank Jacques Amar for useful comments on the manuscript and Mehran Kardar and Terry Hwa for helpful correspondences.

APPENDIX: RESPONSE FUNCTION FOR THE LINEARIZED THEORY

From (19) for the response function $g_E(\tau)$, we need to calculate the cumulant $\sum_{\mathbf{k},\mathbf{q}}\langle|h(\mathbf{k},t)|^2|h(\mathbf{q},t')|^2\rangle_c$, where

$$|h(\mathbf{k},t)|^2=e^{-2t(\nu_\parallel k_\parallel^2+\nu_\perp k_\perp^2)}\int_0^t ds_1\int_0^t ds_2 e^{(\nu_\parallel k_\parallel^2+\nu_\perp k_\perp^2)(s_1+s_2)}\hat{\eta}(\mathbf{k},s_1)\hat{\eta}(-\mathbf{k},s_2)\ .$$

Therefore, we have

$$\sum_{\mathbf{k},\mathbf{q}}\langle|h(\mathbf{k},t)|^2|h(\mathbf{q},t')|^2\rangle=\sum_{\mathbf{k},\mathbf{q}}e^{-2(\nu_\parallel k_\parallel^2+\nu_\perp k_\perp^2)t}e^{-2(\nu_\parallel q_\parallel^2+\nu_\perp^2)t'}\int_0^t ds_1\int_0^t ds_2\int_0^{t'}d\sigma_1\int_0^{t'}d\sigma_2 e^{(\nu_\parallel k_\parallel^2+\nu_\perp k_\perp^2)(s_1+s_2)}$$
$$\times e^{(\nu_\parallel q_\parallel^2+\nu_\perp q_\perp^2)(\sigma_1+\sigma_2)}$$
$$\times\langle\hat{\eta}(\mathbf{k},s_1)\hat{\eta}(-\mathbf{k},s_2)\hat{\eta}(\mathbf{q},\sigma_1)\hat{\eta}(-\mathbf{q},\sigma_2)\rangle.$$

Using (20), only pairwise combinations of η's in the expectation are finite and we have, for $t>t'$,

$$\sum_{\mathbf{k},\mathbf{q}}\langle|h(\mathbf{k},t)|^2|h(\mathbf{q},t')|^2\rangle=\left[D\sum_{\mathbf{k}}e^{-2(\nu_\parallel k_\parallel^2+\nu_\perp k_\perp^2)t}\int_0^t ds\, e^{2(\nu_\parallel k_\parallel^2+\nu_\perp k_\perp^2)s}\right]\left[D\sum_{\mathbf{q}}e^{-2(\nu_\parallel q_\parallel^2+\nu_\perp q_\perp^2)t'}\int_0^{t'}ds\, e^{2(\nu_\parallel q_\parallel^2+\nu_\perp q_\perp^2)s}\right]$$
$$+2D^2\sum_{\mathbf{k}}e^{-2(\nu_\parallel k_\parallel^2+\nu_\perp k_\perp^2)(t+t')}\int_0^{t'}ds_1\int_0^{t'}ds_2 e^{-2(\nu_\parallel k_\parallel^2+\nu_\perp k_\perp^2)(s_1+s_2)}\ .$$

The first term in the last equation drops out when we take the cumulant, which means dropping all products of lower order, and we have for $t>t'$

$$\sum_{\mathbf{k},\mathbf{q}}\langle |h(\mathbf{k},t)|^2|h(\mathbf{q},t')|^2\rangle_c = 2D^2\sum_{\mathbf{k}} e^{-2(\nu_\parallel k_\parallel^2+\nu_\perp k_\perp^2)(t+t')}\left\{\int_0^{t'} ds\, e^{2(\nu_\parallel k_\parallel^2+\nu_\perp k_\perp^2)s}\right\}^2$$

$$= 2D^2\sum_{\mathbf{k}} e^{-2(\nu_\parallel k_\parallel^2+\nu_\perp k_\perp^2)(t+t')}\left\{\frac{1-e^{2(\nu_\parallel k_\parallel^2+\nu_\perp k_\perp^2)t'}}{2(\nu_\parallel k_\parallel^2+\nu_\perp k_\perp^2)}\right\}^2$$

$$= 2D^2\sum_{\mathbf{k}} \frac{1}{4(\nu_\parallel k_\parallel^2+\nu_\perp k_\perp^2)^2}\{e^{-2(\nu_\parallel k_\parallel^2+\nu_\perp k_\perp^2)(t+t')} - 2e^{-2(\nu_\parallel k_\parallel^2+\nu_\perp k_\perp^2)t} + e^{-2(\nu_\parallel k_\parallel^2+\nu_\perp k_\perp^2)(t-t')}\}\ .$$

In the limit $t\to\infty$, $t'\to\infty$, $t>t'$, only the last term survives, and we have

$$\sum_{\mathbf{k},\mathbf{q}}\langle |h(\mathbf{k},t)|^2|h(\mathbf{q},t')|^2\rangle_c = \frac{D^2}{2}\sum_{\mathbf{k}} \frac{1}{(\nu_\parallel k_\parallel^2+\nu_\perp k_\perp^2)^2} e^{-2(\nu_\parallel k_\parallel^2+\nu_\perp k_\perp^2)(t-t')}$$

$$= S_{d'-1}D^2\left[\frac{L}{2\pi}\right]^{d'}\int_{L^{-1}}^{\infty} k^{d'-1}dk\int_0^{\pi/2} d\theta \frac{\sin^{d'-2}\theta}{(\nu_\parallel\cos^2\theta+\nu_\perp\sin^2\theta)^2k^4} e^{-2(\nu_\parallel\cos^2\theta+\nu_\perp\sin^2\theta)k^2(t-t')}\ ,$$

which is Eq. (21).

---

*Present address: Physics Department, Southern University, Baton Rouge, LA 70813.

[1] P. Bak, C. Tang, and K. Wiesenfeld, Phys. Rev. Lett. **59**, 381 (1987).
[2] P. Bak, C. Tang, and K. Wiesenfeld, Phys. Rev. A **38**, 364 (1988).
[3] L. P. Kadanoff, S. R. Nagel, L. Wu, and S.-M. Zhou, Phys. Rev. A **39**, 6524 (1989).
[4] D. Dhar and R. Ramaswamy, Phys. Rev. Lett. **63**, 1659 (1989).
[5] T. Hwa and M. Kardar, Phys. Rev. Lett. **62**, 1813 (1989).
[6] K. Kawasaki, in *Phase Transition and Critical Phenomena*, edited by C. Domb and M. S. Green (Academic, London, 1976), Vol. 5a, p. 166, and references therein.
[7] V. Yakhot and Z.-S. She, Phys. Rev. Lett. **60**, 1840 (1988).
[8] L.-H. Tang, T. Nattermann, and B. M. Forest, Phys. Rev. Lett. **65**, 2422 (1990).
[9] J. G. Amar and F. Family, Phys. Rev. A **45**, R3373 (1992); **45**, 5378 (1992).
[10] T. Hwa and M. Kardar (unpublished).
[11] H. J. Jensen, K. Christensen, and H. C. Fogedby, Phys. Rev. B **40**, 7425 (1989).